PHYSICAL REVIEW A VOLUME 49, NUMBER 3 MARCH 1994

Differential cross sections and angular-correlation parameters for the excitation of hydrogen atoms to $n = 3$ and $n = 2$ states by electron impact between 16 and 100 eV

Y. D. Wang* and J. Callaway†
Department of Physics and Astronomy, Louisiana State University, Baton Rouge, Louisiana 70803-4001

K. Unnikrishnan
Department of Theoretical Physics, Institute of Advanced Studies, Australian National University, Canberra, Australian Capital Territory 0200, Australia

(Received 25 October 1993)

Differential cross sections and angular-correlation parameters relating to elastic scattering and electron-impact excitation of hydrogen atoms to the $n = 3$ and $n = 2$ states are presented for energies of 16, 20, 35, 54, and 100 eV. Results are obtained from a close-coupling calculation using a 17-state target basis including seven exact states and ten pseudostates. Comparisons are made with experiment and with other calculations.

PACS number(s): 34.80.Dp

I. INTRODUCTION

In recent work, we have reported calculations of the total cross section, and of integrated cross sections for elastic scattering, and excitation of hydrogen atoms to the $n = 2$ and 3 states by intermediate energy electrons (14–100 eV) [1]. These cross sections were used to obtain improved results for effective (thermally averaged) collision strengths for $n = 3$ excitations. In this paper, we present results for differential cross sections and for some parameters involved in the description of the angular correlation between electron scattering and photon emission. We report and compare with experiment our results for the quantities involved with elastic scattering and $n = 2$ excitations, however, we would like to emphasize here results concerned with $n = 3$ excitations which have not been intensively studied.

Although theoretical studies of the scattering of electrons by hydrogen atoms have about a 60 year history, it is only relatively recently that accurate results have been obtained in the intermediate energy range (roughly defined to include energies from the ionization threshold up to 100 eV) [2–5]. The calculations reported in [2–5] are in reasonable agreement with each other in regard to elastic scattering and the excitation of the $n = 2$ states. Agreement with experiment is reasonably good, although there are some difficulties with regard to certain angular-correlation parameters. (Specifics will be discussed below). Much less has been reported concerning $n = 3$ excitations, at a similar (presumed) level of accuracy. In addition to the work of [1], there is now a letter describing a similar calculation of integrated cross sections using the "intermediate energy R matrix method" [6].

When we began these calculations, there were no published reports of experimental measurements of differential cross sections for n=3 excitations although there had been some work on electron-photon angular correlations [7–9]. We have previously presented our predictions for these quantities in the narrow energy range between the $n = 3$ and $n = 4$ thresholds [10], and here consider energies up to 100 eV. We hoped that the availability of specific predictions would serve as a stimulus to measurements. In order to make plausible to the reader our claim that the results presented here are likely to be of high quality, we compare our calculation for $n = 2$ excitations with the existing experiments. In these cases, it will be seen that there are only few and minor differences between the present results for these transitions and the results of other high quality calculations in which $n = 2$ transitions have been emphasized [3–5], although there are still some disagreements between all the calculations cited and experiment. Atomic units with energy in rydbergs are used unless otherwise stated.

II. METHOD

We summarize here very briefly the essential features of our computations. A more detailed account is given in [1]. Our calculations are of the close coupling type, in which we use a 17-state target basis. This basis contains seven exact atomic states ($1s$, $2s$, $2p$, $3s$, $3p$, $3d$, and $4f$) and ten pseudostates (5 s-like, 3 p-like, 2 d-like). The parameters of the Slater-type orbitals (STO) from which the pseudostates are constructed were chosen with the intent of describing short and intermediate range correlations, and are intended to be used above the ionization threshold. This set will not be optimum in the resonance region. The target states themselves are found by diagonalizing the Hamiltonian of an isolated atom in the finite basis. In this way, a set of target states is obtained which includes some exact states and some pseudostates. The orbital parameters and the energies of the states are given in Table I of [1]. Here, we present results at incident energies of 1.21, 1.44, 2.60, 4.00, and 7.35 Ry (16.5, 19.6, 35.4, 54.4, and 100 eV).

*Electronic address: ydwang@rouge.phys.lsu.edu
†Electronic address: callaway@rouge.phys.lsu.edu

The use of a small set of discrete pseudostates to represent the continuum can lead to unphysical structure in the cross sections at energies close to the thresholds of the pseudostates, often referred to as pseudoresonances. We remove this by a procedure, described in [11], in which a least squares fit is made to the complex transition amplitudes for fixed L and S with a low order polynomial in energy. This was done for angular momenta $0 \leq L \leq 5$. It did not appear to be necessary for $L \geq 6$. In addition, our basis set has no thresholds near $k^2 = 4.0$ and $k^2 = 7.35$ Ry, so averaging did not have to be performed at these energies.

At the lower two energies we considered ($k^2 = 1.21$ and 1.44 Ry), the transition amplitudes converge rapidly enough with increasing total angular momentum L that it was possible to carry the close coupling calculations to large enough L so that the differential cross sections and other quantities of interest converged. At higher energies, it was necessary to go beyond the range of L's for which detailed calculations were performed. Our method for doing this is based on the observation that the dominant L dependence of the elements of the reaction (K) matrix connecting the $1s$ with p states is, according to the Born approximation [12], $(\frac{k_f}{k_i})^L$. Therefore, we extrapolate the $1s$-np amplitudes as a geometric series. The $1s$-ns amplitudes converge rapidly and do not require extrapolation. We assume that the $1s$-$3d$ amplitude may be extrapolated similarly to those for p states.

III. RESULTS

A. Elastic scattering and excitation of $n = 2$

Calculations of differential cross sections and related quantities readily generate large arrays of numbers. These arrays become even more extensive when state multipoles, which are of particular interest in coincidence and correlation measurements, are considered. It is possible to present only a representative sample of these results in a journal publication. We give tabulated numerical data at $k^2 = 4.0$ Ry only. For those readers who may be interested in a more complete presentation of our results than can be made in these papers, we will supply (either in computer printed form, or by electronic mail) tables of differential cross sections and/or transition amplitudes as functions of electron scattering angle at each of the energies considered here. Tables and figures of transition amplitudes, differential cross sections, and spin-asymmetry parameters in microfiche form can also be obtained from the Physics Auxiliary Publication Service of the American Institute of Physics [32].

Most of the experimental investigations of electron-hydrogen scattering have, apart from ionization, concerned either elastic scattering or excitation of the $n = 2$ states ($2s$, $2p$). In order that the reader can properly gauge the quality of the present calculation, and appreciate the current situation in regard to comparison of theory and experiment, we describe our results concerning these processes below.

Theoretical calculations of the close coupling type have yielded rather good agreement with elastic scattering experiments for many years, provided that pseudostates which reproduce the atomic polarizability are included in the target basis. Alternately, one can use an optical potential which incorporates an energy dependent effective polarization potential. Because elastic scattering is extensively discussed in the literature, we think this topic needs only a brief mention here, and that graphical representation will suffice. The present results are shown in Fig. 1, where they are compared with experiment [13,14] and, at three energies, with the calculations of [5]. It will be noted that the differences between the present work and the calculations of [5] are quite small. There are measurements of the spin asymmetry in elastic scattering at a single angle (90°) for a few energies [15]. The present results agree well with our previous calculation [16], which is in reasonable agreement with experiment. We do not show details here.

Next, we discuss transitions to the $n = 2$ states. There are measurements of the differential cross section for excitation of the combined $n = 2$ states for incident energies of 1.21 and 1.44 Ry [17]. Our results are shown pictorially in Figs. 2 and 3. The differential cross sections are in fairly good agreement with experiment although there are some disagreements at backward angles.

At $k^2 = 1.21$ Ry, our results can also be compared with calculations of Scholz *et al.* [18] and Fon, Aggarwal, and Ratnavelu [19]. Scholz *et al.* used the intermediate

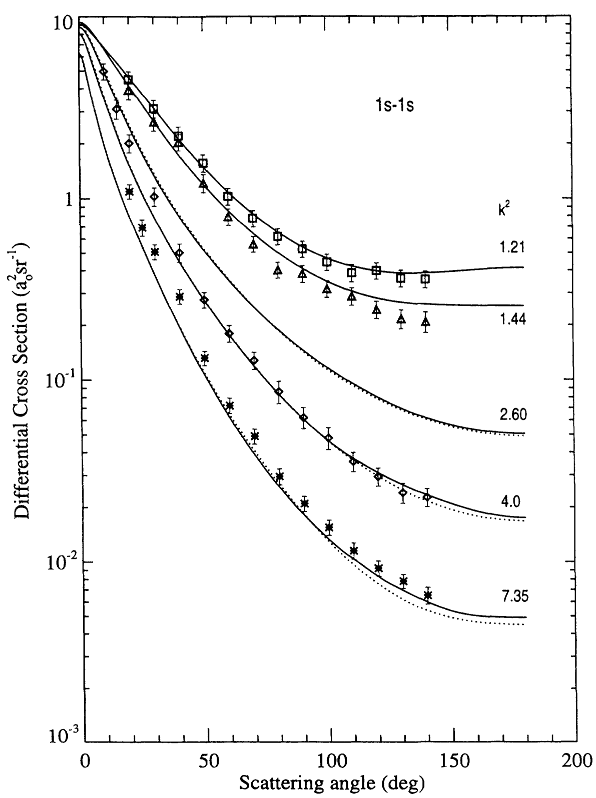

FIG. 1. Differential cross sections for elastic scattering from the ground state. Solid line, present results; dotted lines, calculation of Bray and Stelbovics [5]. Symbols with error bars represent measurements of Williams [13,14]. We are not aware of measurements near $k^2 = 2.60$ Ry.

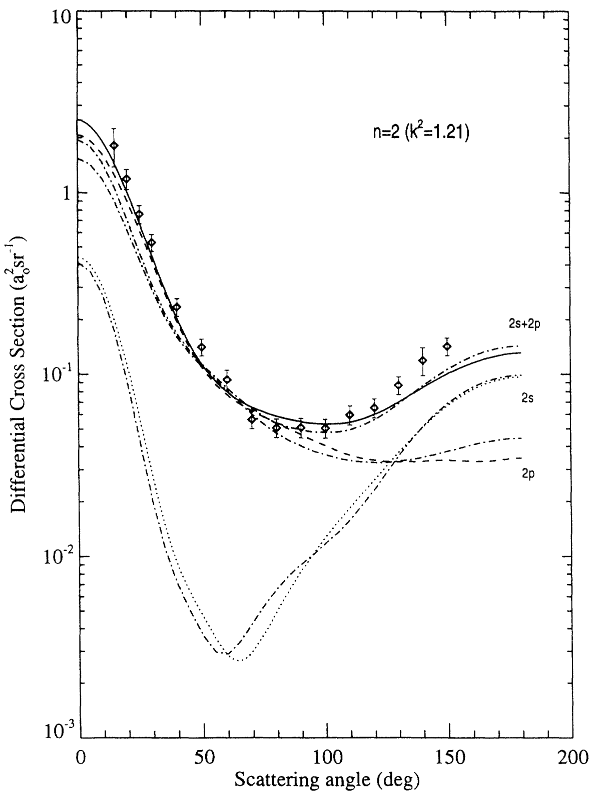

FIG. 2. Differential cross section for excitation of $n = 2$ states for an incident energy of 1.21 Ry. Dotted line, 2s; dashed line, $2p$; solid line, total $n = 2$; symbols, measurements of Williams [17] for total $n = 2$; dashed-dot curves are corresponding results from Scholz *et al.* [18].

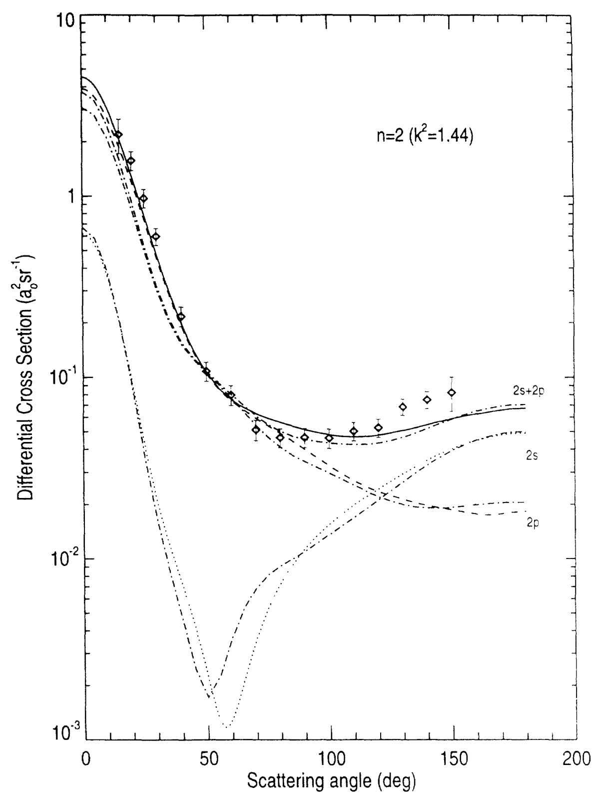

FIG. 3. Similar to Fig. 2 but for 1.44 Ry.

energy R matrix method for $0 \leq L \leq 4$ and a 9-state basis (3 exact and 6 pseudostates) for $L \geq 5$. In contrast, the results of Fon, Aggarwal, and Ratnavelu are obtained using a basis of 15 exact bound states (all states through $n = 5$). At $k^2 = 1.44$ Ry, we compare with the results of Scholz *et al.* [18]. The differential cross sections of Fon, Aggarwal, and Ratnavelu at $k^2 = 1.21$ Ry are larger than ours at all angles. For the $2s$ state, the difference is greater than a factor of 2 at some angles ($30° - 45°$), but considerably smaller ($10\% - 20\%$) for the 2p state over most of the range. Their work is expected to produce larger cross sections than ours because they do not include any pseudostates to represent the continuum. Our agreement with Scholz *et al.* is much better, particularly for the $2s$ state, at both energies. Our differential cross sections for $2p$ excitation are in reasonable agreement at backward angles but are up to 30% larger in the forward direction at both energies. Unfortunately, the precision of the experimental data is too low to enable one to conclude which calculation is preferable.

At $k^2 = 2.60$ Ry, there are no differential cross section measurements but two of the three angular correlation parameters, $\lambda = \sigma_0/(\sigma_0 + 2\sigma_1)$ and $R = \mathrm{Re}\langle a_1 a_0^* \rangle/(\sigma_0 + 2\sigma_1)$ have been reported [20]. Here σ_m is the differential cross section and a_m is the complex amplitude for the excitation of the $2p_m$ state and $\langle\,\rangle$ denotes a spin average of the product of two scattering amplitudes. Our results

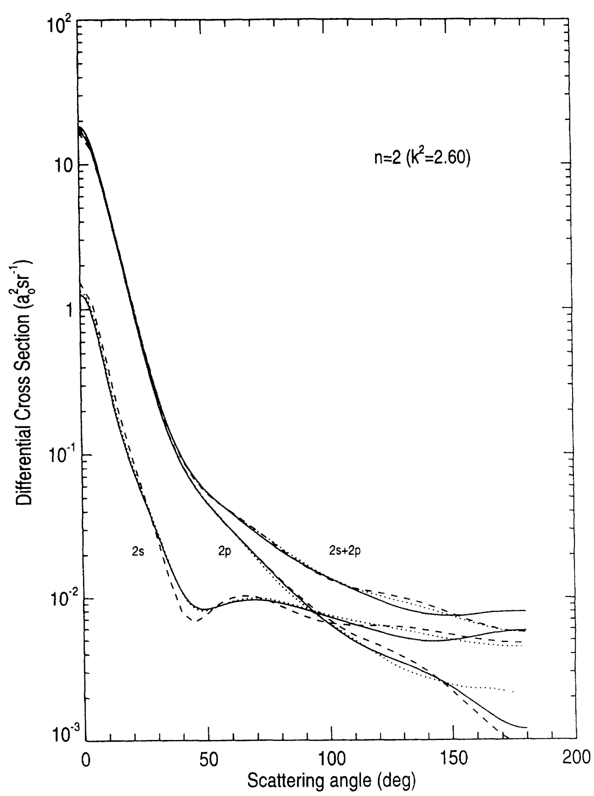

FIG. 4. Differential cross section for excitation of $n = 2$ states at $k^2 = 2.60$ Ry. Solid curves, present results; dotted curve, Bray and Stelbovics [5]; dashed curve, Scholz *et al.* [18].

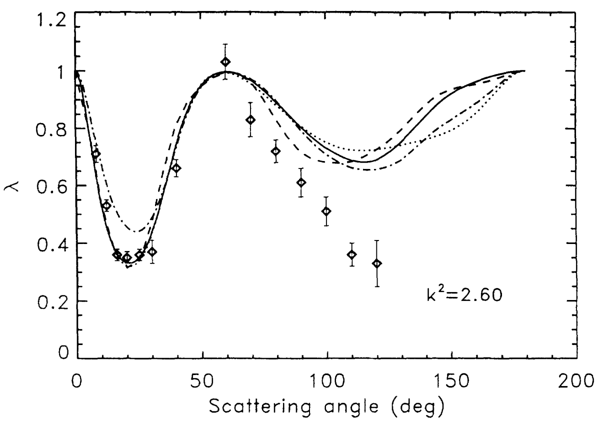

FIG. 5. λ parameter for $2p$ excitation. Solid curve, our results for $k^2 = 2.60$ Ry (35.4 eV). Dashed curve, results of Scholz *et al.* [18]; dotted curve, Bray and Stelbovics [5] (35.0 eV). Symbols, measurements of Slevin *et al.* [20] (35.0 eV). Dashed-dot curve shows our λ for $3p$ excitation.

for differential cross sections are shown in Fig. 4. Results for λ and R are shown in Figs. 5 and 6. We have included curves for $3p$ excitation in these figures.

Note that the theoretical curves, based on the present calculation and those of Scholz *et al.* [18] and of Bray and Stelbovics [5] are in substantial agreement with each others. There are only minor differences at large angles. However, there are significant differences between theory and experiment, most importantly in regard to the λ parameter for angles above 60° which the present calculation does nothing to resolve. We have included our results for $3p$ excitation in these figures to illustrate the point that the correlation parameters show only rather small differences between $2p$ and $3p$ excitation.

Next, we consider an incident energy of $k^2 = 4.0$ Ry (54.4 eV). This is the energy at which the most complete experimental measurements have been made [21–24], and it is the energy for which we give numerical results in this paper. Our results for the differential cross section and the angular-correlation parameters are shown pictorially in Figs. 7–10. Here we also show the parameter $I = \mathrm{Im}\langle a_1 a_0^* \rangle / (\sigma_0 + 2\sigma_1)$. Numerical results are given in Table I. As was found at 35 eV, the results of the present calculation and those of Scholz *et al.* [18] and Bray and Stelbovics [5] are in rather good agreement. We also agree quite well with the open pseudostate calculation of

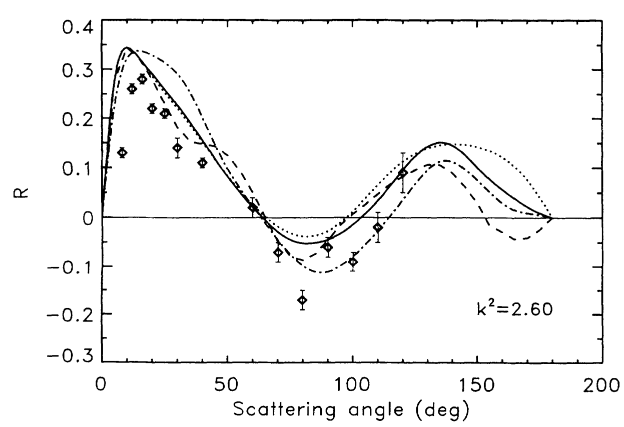

FIG. 6. Similar to Fig. 5, but for the R parameter.

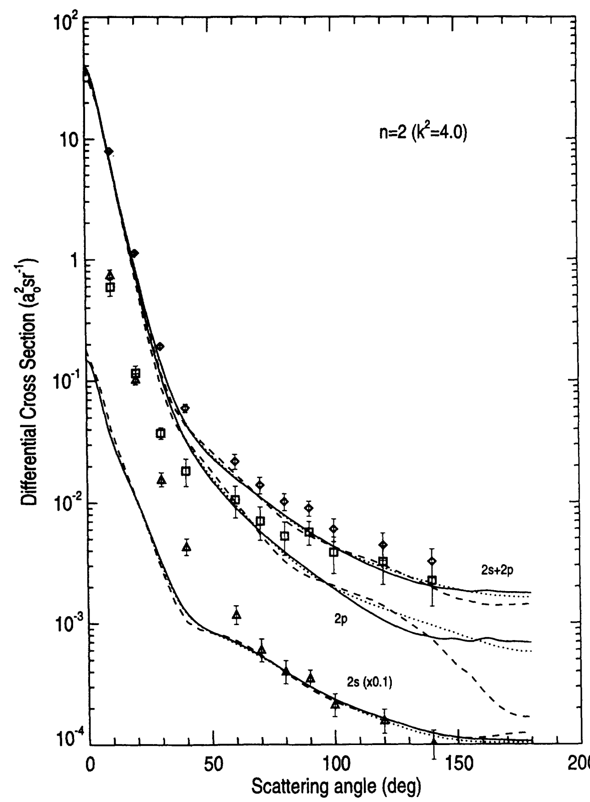

FIG. 7. Similar to Fig. 4 but for $k^2 = 4.0$ Ry. Symbols are measurements of Williams [21].

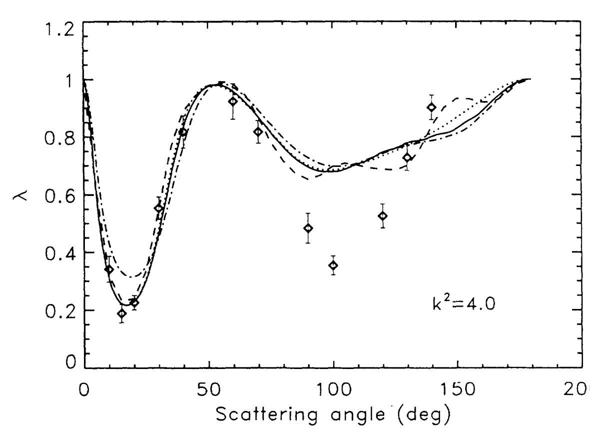

FIG. 8. λ parameter for $2p$ excitation at $k^2 = 4.0$ Ry. Solid curve, present results; dotted curve, Bray and Stelbovics [5]; dashed curve, Scholz *et al.* [18]; dashed-dot curve, present results for $3p$ excitation; symbols, measurements of Williams [21].

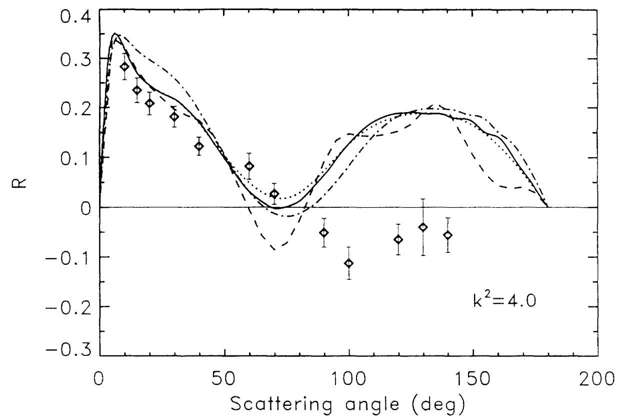

FIG. 9. Similar to Fig. 8, but for the R parameter.

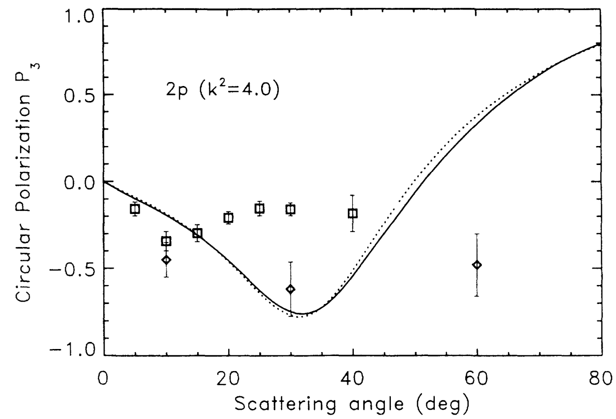

FIG. 11. Theoretical and experimental data for the circular polarization $\bar{P}_3$ at an incident energy of $k^2 = 4.0$ Ry. Solid line, present calculation; dotted line, Bray and Stelbovics [5]. Symbols: squares, measurements of Chormaic, Chwirot, and Levin [26]; diamonds, data deduced from measurements of Williams [21,22].

van Wyngaarden and Walters [25]. Agreement with experiment is rather good near the forward direction, but deteriorates at backward angles. The most significant discrepancies involve all of the correlation functions at backward angles. The figures show the experimental results of Williams [21,22]; those of Weigold, Frost, and Nyguard [23] have larger error bars, but agree well with those of Williams. Thus we confront an impasse in which four recent independent calculations employing quite different methods agree well with each other, but disagree significantly with two independent experiments, which also agree with each other.

As a further experimental input, Chormaic, Chwirot, and Slevin [26] recently reported measurements on the circular polarization, $\bar{P}_3$, and on $\mathcal{P}^+$, a parameter introduced by Andersen, Gallagher, and Hertel [27] whose value can be used to assess the spin-exchange effect in the excitation process. The circular polarization parameter is proportional to I, $\bar{P}_3 = 2\sqrt{2}I$. The coherence parameter $\mathcal{P}^+$ is related to the λ, R, and I parameters, $\mathcal{P}^{+2} = (2\lambda - 1)^2 + 8(R^2 + I^2)$. $\mathcal{P}^+$ has a value of less than or equal to 1. A value closer to 1 is an indication of weaker exchange interaction. In Figs. 11 and 12, we compare two calculations with two experiments. The calculations of Bray and Stelbovics were deduced from [5]. The measurements are from Chormaic, Chwirot, and Slevin [26] and from Williams [21,22]. Apparently, there is little agreement between theories and experiments. While the two experiments point to the presence of significant exchange interactions in the excitation, the two theories reveal the contrast.

Our results at $k^2 = 7.35$ Ry for $2s$, $2p$, and total $n = 2$ differential cross sections are given in Fig. 13. These quantities, as well as the correlation parameters, agree satisfactorily with those of Bray and Stelbovics [5] and van Wyngaarden and Walters [25]. Scholz *et al.* [18] do not consider this energy. The measurements of Williams and Willis [28] determine only the sum of the $2s$ and $2p$ cross sections. Our results, as well as those of Bray and Stelbovics [5], lie significantly below the experimental points except at forward angles. Comparison of the

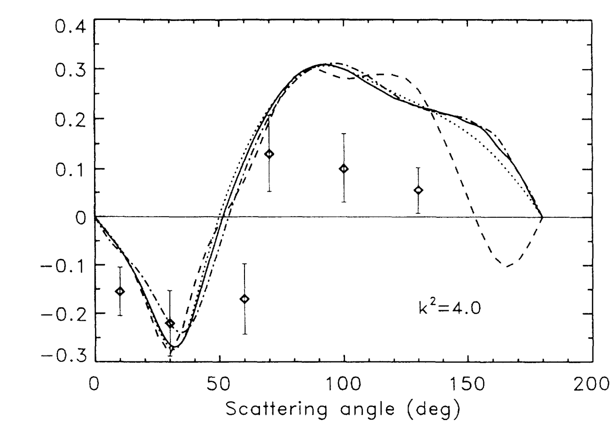

FIG. 10. Similar to Fig. 9, but for the I parameter. The measurements are from Williams [22].

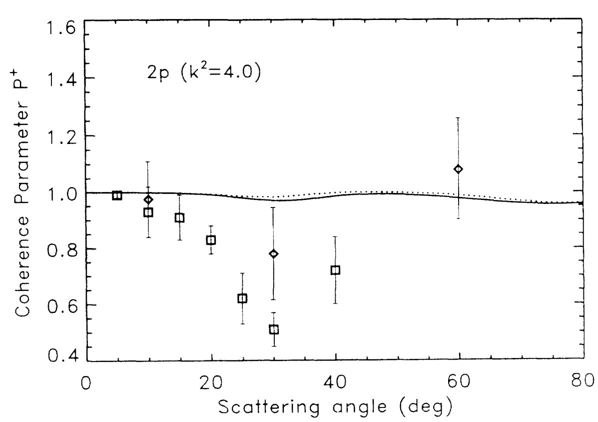

FIG. 12. Similar to Fig. 11 but for the coherence parameter $\mathcal{P}^+$.

TABLE I. Differential cross sections (in units of $a_0^2\,\mathrm{sr}^{-1}$) for $1s-2s$, $1s-2p$ transitions at an incident electron energy of $k^2 = 4.0$ Ry. Integrated cross sections (in units of πa_0^2), σ_{2s}, and σ_{2p} as well as alignment parameters for $2p$ state λ, R, and I are also given. The numbers in brackets denote multiplicative powers of ten.

θ (deg)	$2s$	$2p$	λ	R	I	θ (deg)	$2s$	$2p$	λ	R	I
0	1.49	3.78[1]	1.000	0.000	0.000	95	2.65[−3]	2.28[−3]	0.681	0.096	0.308
5	8.12[−1]	1.97[1]	0.598	0.345	−0.035	100	2.37[−3]	1.92[−3]	0.679	0.126	0.300
10	3.38[−1]	6.52	0.309	0.319	−0.068	105	2.13[−3]	1.63[−3]	0.687	0.152	0.287
15	1.83[−1]	2.17	0.221	0.271	−0.109	110	1.94[−3]	1.39[−3]	0.705	0.171	0.271
20	1.06[−1]	7.50[−1]	0.230	0.245	−0.161	115	1.78[−3]	1.20[−3]	0.723	0.183	0.257
25	5.85[−2]	2.75[−1]	0.308	0.228	−0.222	120	1.64[−3]	1.04[−3]	0.746	0.188	0.242
30	3.16[−2]	1.13[−1]	0.467	0.217	−0.265	125	1.51[−3]	9.35[−4]	0.759	0.190	0.234
35	1.82[−2]	5.57[−2]	0.665	0.197	−0.257	130	1.41[−3]	8.48[−4]	0.778	0.188	0.224
40	1.22[−2]	3.29[−2]	0.833	0.170	−0.192	135	1.32[−3]	7.97[−4]	0.786	0.188	0.218
45	9.70[−3]	2.21[−2]	0.932	0.136	−0.106	140	1.24[−3]	7.56[−4]	0.800	0.183	0.212
50	8.51[−3]	1.59[−2]	0.974	0.098	−0.022	145	1.19[−3]	7.35[−4]	0.811	0.178	0.205
55	7.69[−3]	1.19[−2]	0.979	0.063	0.052	150	1.14[−3]	7.31[−4]	0.828	0.171	0.193
60	6.91[−3]	9.16[−3]	0.958	0.031	0.116	155	1.11[−3]	7.03[−4]	0.856	0.150	0.184
65	6.12[−3]	7.20[−3]	0.918	0.011	0.171	160	1.10[−3]	7.35[−4]	0.885	0.142	0.158
70	5.35[−3]	5.77[−3]	0.868	−0.002	0.217	165	1.09[−3]	7.26[−4]	0.928	0.110	0.128
75	4.63[−3]	4.71[−3]	0.815	0.001	0.254	170	1.08[−3]	6.96[−4]	0.964	0.073	0.097
80	4.00[−3]	3.89[−3]	0.765	0.012	0.282	175	1.07[−3]	6.98[−4]	0.991	0.037	0.047
85	3.46[−3]	3.24[−3]	0.725	0.037	0.299	180	1.07[−3]	6.87[−4]	1.000	0.000	0.000
90	3.02[−3]	2.72[−3]	0.696	0.064	0.308						
σ_{2s}	6.17[−2]										
σ_{2p}	7.46[−1]										
Sum	8.08[−2]										

calculations of van Wyngaarden and Walters with experiment shows a very similar pattern of agreement and disagreement.

B. Excitation of $n = 3$ states

First, we would like to present in Table II, primarily for the benefit of theorists who would like to compare results of other calculations with ours, a small sample of the complex amplitudes for $1s \to n = 3$ transitions for small values of the angular momentum L (0, 1, 2) and both spin states (0, 1). These amplitudes (denoted f_{mn}) are related to the elements of the S matrix by

$$S_{mn} = \delta_{mn} + 2if_{mn} \tag{1}$$

TABLE II. Amplitudes (real and imaginary parts) for $1s \to n = 3$ transitions for the first three partial waves. The numbers in brackets denote multiplicative powers of ten.

L	S	Channel	$E = 1.21$		$E = 1.44$		$E = 2.60$		$E = 4.0$		$E = 7.35$	
0	0	$3s$	1.19[−2]	−6.89[−2]	−3.69[−2]	−6.76[−2]	−2.85[−2]	3.94[−2]	−4.32[−3]	4.24[−2]	1.35[−2]	3.73[−2]
0	0	$3p$	−4.92[−2]	2.07[−2]	−4.98[−2]	7.65[−2]	3.61[−2]	7.03[−2]	3.54[−2]	5.01[−2]	2.59[−2]	3.28[−2]
0	0	$3d$	−1.42[−2]	−3.71[−2]	−2.82[−2]	−3.29[−2]	−2.69[−2]	4.90[−3]	−7.14[−3]	7.45[−3]	8.65[−4]	8.74[−3]
0	1	$3s$	1.10[−2]	−5.70[−3]	7.60[−3]	−1.30[−2]	−1.78[−2]	−2.20[−3]	−1.45[−2]	1.63[−2]	−2.57[−3]	2.80[−2]
0	1	$3p$	−1.08[−2]	−7.50[−3]	−2.09[−2]	−1.00[−3]	−1.52[−2]	3.67[−2]	2.76[−4]	4.08[−2]	1.16[−2]	2.93[−2]
0	1	$3d$	4.00[−3]	−4.30[−3]	2.00[−3]	−8.10[−3]	−8.60[−3]	−5.50[−3]	−6.55[−3]	1.32[−3]	−1.53[−3]	5.96[−3]
1	0	$3s$	−4.00[−4]	1.53[−2]	1.14[−2]	2.61[−2]	3.10[−2]	3.51[−2]	3.78[−2]	2.97[−2]	3.45[−2]	2.30[−2]
1	0	$3p$-1	−3.24[−2]	4.34[−2]	−9.70[−3]	6.29[−2]	2.92[−2]	3.73[−2]	2.55[−2]	2.01[−2]	1.45[−2]	1.21[−2]
1	0	$3p$+1	4.42[−2]	2.00[−2]	4.78[−2]	1.30[−2]	3.40[−2]	−3.90[−3]	2.54[−2]	8.66[−4]	1.59[−2]	5.30[−3]
1	0	$3d$-2	−2.14[−2]	−3.82[−2]	−3.26[−2]	−2.63[−2]	−1.70[−2]	5.10[−3]	−4.24[−3]	6.38[−3]	1.91[−3]	5.85[−3]
1	0	$3d$+2	−1.56[−2]	1.39[−2]	−1.13[−2]	1.35[−2]	−4.70[−3]	8.70[−3]	2.76[−3]	3.81[−3]	6.29[−3]	4.03[−3]
1	1	$3s$	−2.21[−2]	7.50[−3]	−1.59[−2]	2.09[−2]	7.40[−3]	2.61[−2]	1.47[−2]	2.60[−2]	2.00[−2]	2.32[−2]
1	1	$3p$-1	1.00[−2]	1.14[−2]	1.16[−2]	5.90[−3]	4.00[−4]	8.60[−3]	2.91[−3]	1.21[−2]	5.69[−3]	1.03[−2]
1	1	$3p$+1	−8.00[−4]	2.27[−2]	9.00[−3]	2.51[−2]	1.78[−2]	1.69[−2]	1.69[−2]	1.24[−2]	1.28[−2]	8.58[−3]
1	1	$3d$-1	−6.90[−3]	1.90[−3]	−5.60[−3]	3.20[−3]	−3.30[−3]	9.00[−4]	−2.01[−3]	1.98[−3]	7.53[−4]	4.01[−3]
1	1	$3d$+1	−7.70[−3]	−5.00[−3]	−9.70[−3]	−2.70[−3]	−4.90[−3]	2.40[−3]	−5.06[−4]	3.91[−3]	3.30[−3]	4.23[−3]
2	0	$3s$	−1.61[−2]	−3.85[−2]	−2.69[−2]	−2.72[−2]	1.21[−2]	2.30[−3]	2.20[−2]	5.44[−3]	2.84[−2]	9.54[−3]
2	0	$3p$-1	−3.10[−3]	6.23[−2]	3.44[−2]	7.25[−2]	5.65[−2].	2.62[−2]	4.67[−2]	1.88[−2]	2.97[−2]	1.32[−2]
2	0	$3p$+1	−1.29[−2]	−2.00[−2]	−1.03[−2]	−1.34[−2]	−1.00[−3]	−8.50[−3]	2.21[−3]	−4.66[−3]	3.59[−3]	−5.46[−4]
2	0	$3d$-2	−3.54[−2]	−2.05[−2]	−4.30[−2]	−4.30[−3]	−1.22[−2]	1.26[−2]	−5.37[−3]	1.08[−2]	4.21[−4]	6.67[−3]
2	0	$3d$	−2.26[−2]	−3.00[−4]	−2.31[−2]	8.10[−3]	−3.40[−3]	1.09[−2]	2.23[−3]	7.07[−3]	4.39[−3]	4.69[−3]
2	0	$3d$+2	7.30[−3]	7.00[−4]	7.40[−3]	−1.70[−3]	3.70[−3]	1.10[−3]	6.37[−3]	3.72[−4]	7.06[−3]	1.13[−3]
2	1	$3s$	5.30[−3]	9.00[−3]	1.07[−2]	9.60[−3]	1.85[−2]	1.12[−2]	2.16[−2]	1.31[−2]	2.33[−2]	1.27[−2]
2	1	$3p$-1	−4.20[−3]	1.53[−2]	3.00[−4]	2.20[−2]	1.57[−2]	2.62[−2]	1.96[−2]	2.12[−2]	1.81[−2]	1.47[−2]
2	1	$3p$+1	1.52[−2]	2.30[−3]	1.69[−2]	2.00[−4]	1.31[−2]	−1.60[−3]	9.92[−3]	−1.13[−3]	6.43[−3]	1.22[−4]
2	1	$3d$-2	−1.30[−2]	−5.40[−3]	−1.38[−2]	−1.70[−3]	−8.20[−3]	4.90[−3]	−2.60[−3]	5.12[−3]	1.15[−4]	5.11[−3]
2	1	$3d$	−3.00[−3]	−4.10[−3]	−4.80[−3]	−3.00[−3]	−3.60[−3]	2.70[−3]	−4.71[−4]	3.55[−3]	2.20[−3]	3.62[−3]
2	1	$3d$+2	−4.10[−3]	3.00[−3]	−3.50[−3]	3.70[−3]	−3.00[−4]	2.40[−3]	2.66[−3]	2.40[−3]	4.74[−3]	2.30[−3]

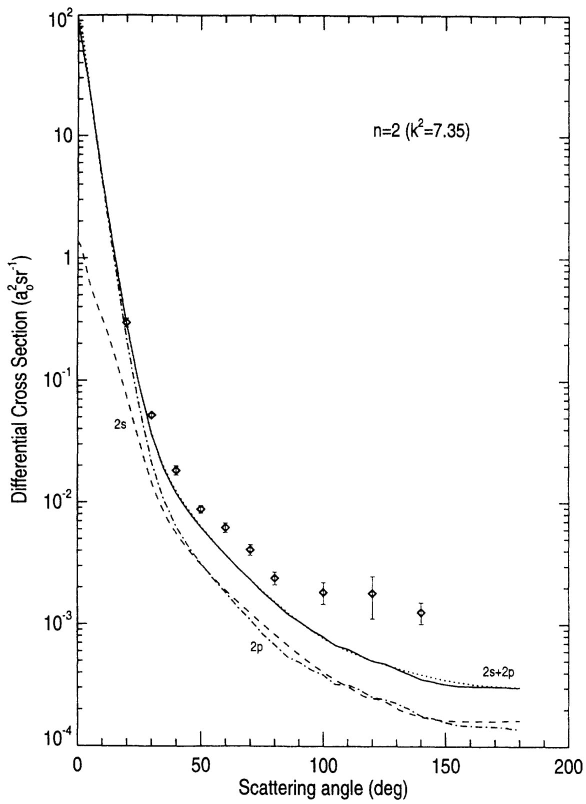

FIG. 13. Differential cross section for $n = 2$ excitation at $k^2 = 7.35$ Ry compared with measurements of Williams and Willis [28]. Present results: solid curve for total $n = 2$; dashed line for $2s$; dashed-dot curve for $2p$. Dotted line is from Bray and Stelbovics [5].

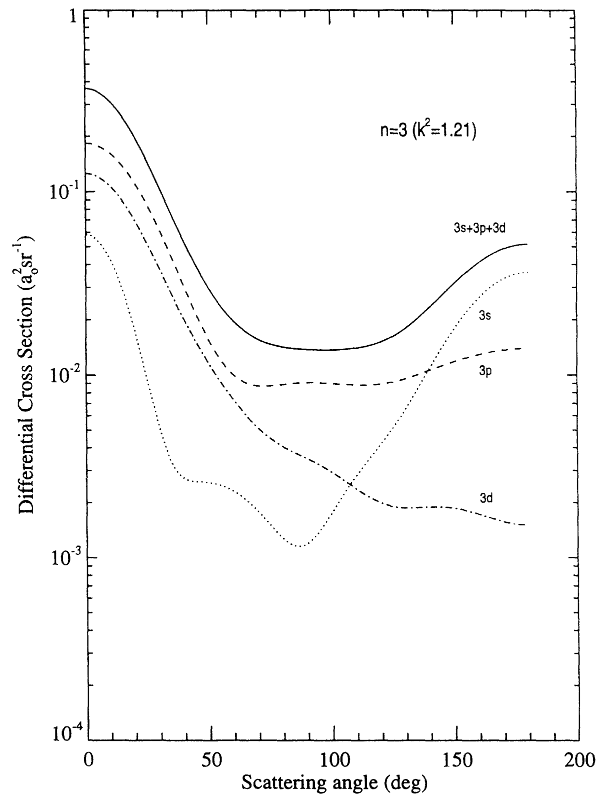

FIG. 14. Differential cross sections for $n = 3$ excitation at $k^2 = 1.21$ Ry. Solid curve, total $n = 3$; dashed curve, $3p$; dashed-dot curve, $3d$; dots, $3s$.

where m and n are channel indices. Note that in Table II, for each transition and each energy, the first number is the real part of the amplitude; the second is the imaginary part. The normalization convention used here is the same as we have employed previously in [11].

At this time, there is very little experimental information on $n = 3$ excitation cross sections. Neither is there agreement on a standard characterization of angular correlations relating to the $3d$ state (compare $2p$ excitation, which is routinely characterized by the three parameters, λ, R, I). On the other hand, the increased angular momentum involved in the $3d$ state increases the possible choices of parameters. In this paper, we show (in Figs. 14–18) the differential cross sections for $3s$, $3p$, and $3d$ excitation as well as their sum.

In general, one sees that as energy increases all the cross sections become more strongly peaked in the forward direction. The $3p$ cross section becomes increasingly dominant in the forward direction while the 3s remains important for backward scattering angles. At $k^2 = 4.0$ Ry, there is a measurement of the cross section for $3p$ excitation by Williams, Stelbovics, and Bray [29]. Those results are included in Fig. 17. These measurements are restricted to angles of 35° and smaller. In this angular range, $3p$ excitation dominates both $3s$ and $3d$, so both the $3p$ and combined $n = 3$ calculated cross sec-

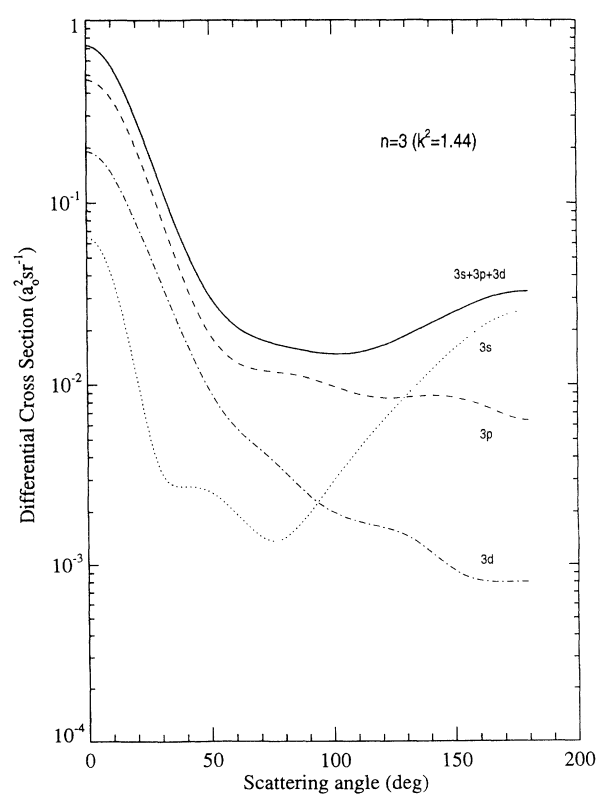

FIG. 15. Similar to Fig. 14, but for $k^2 = 1.44$ Ry.

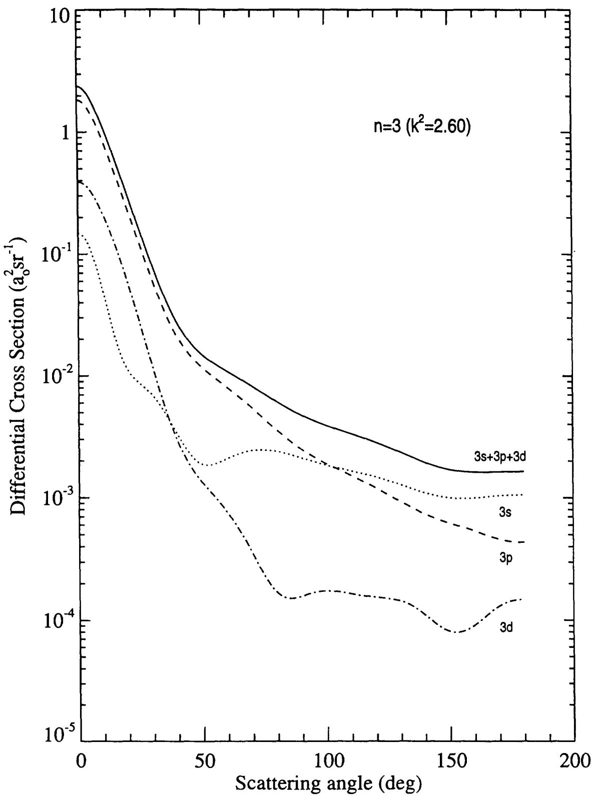

FIG. 16. Similar to Fig. 14, but for $k^2 = 2.60$ Ry.

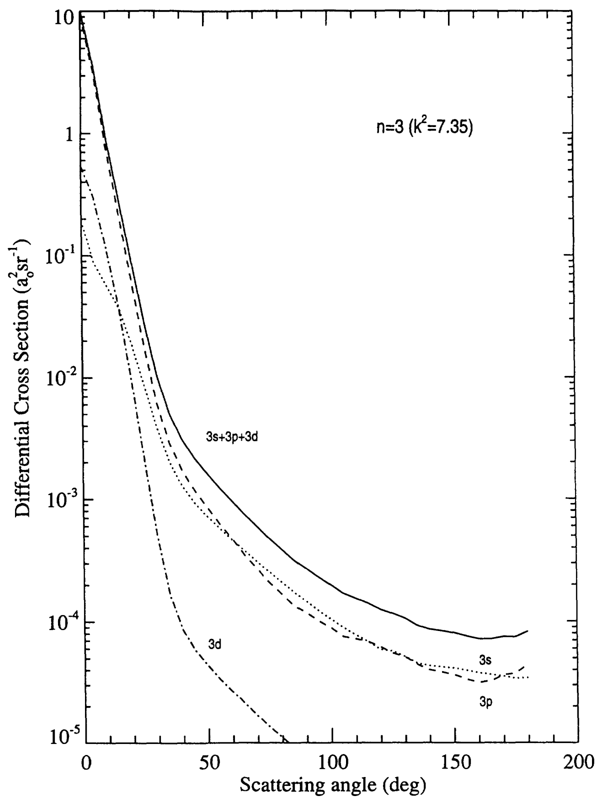

FIG. 18. Similar to Fig. 14, but for $k^2 = 7.35$ Ry.

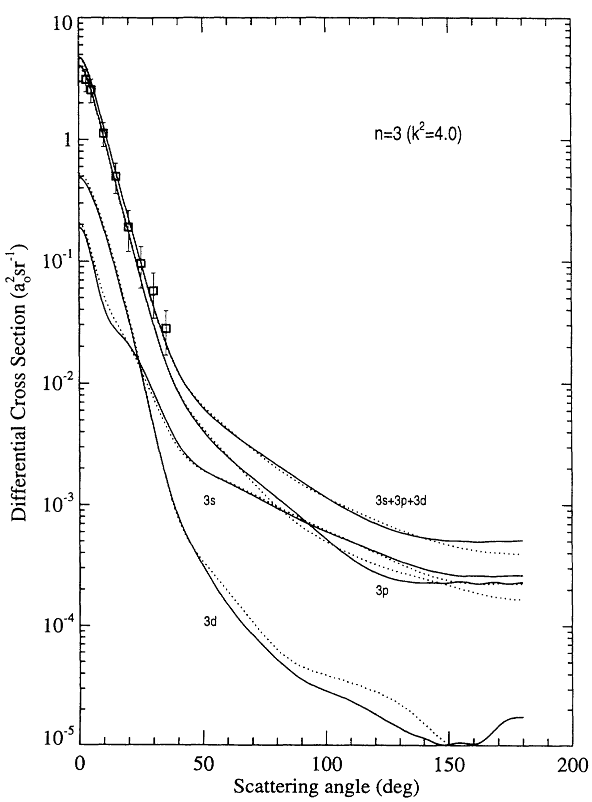

FIG. 17. Differential cross sections for $n = 3$ excitation at $k^2 = 4.0$ Ry. Solid curves, present results; dotted curve and symbols for measurements are from Williams, Stelbovics, and Bray [29]. The measurements are for $3p$ only.

tions are within the error bars at several angles. This is also the single energy at which comparison can be made with another theoretical calculation, and as is indicated in the figure, there is good agreement with the calculations of Williams, Stelbovics, and Bray [29]. Numerical results for $3s$, $3p$, and $3d$ differential cross sections are tabulated in Table III.

In addition, we present the λ, R, and I parameters for $3p$ excitation in Figs. 19–21, and for $k^2 = 4.0$ Ry, in

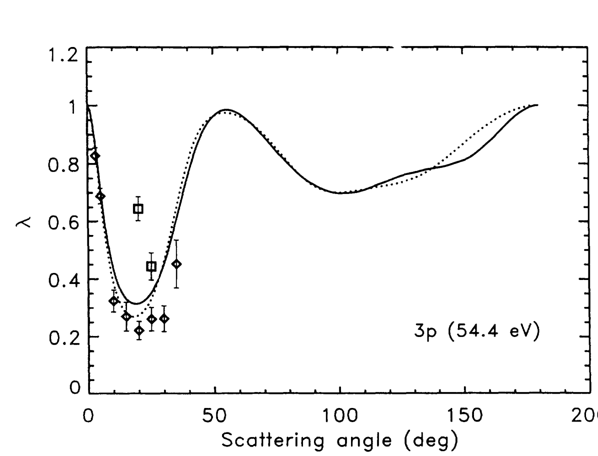

FIG. 19. λ parameter for $3p$ excitation at $k^2 = 4.0$ Ry. Solid curve, present results; dotted curve, theory of Ref. [29]. Symbols: diamonds, measurements of Williams, Stelbovics, and Bray [29]; squares, measurements of Chwirot and Slevin [7].

TABLE III. Differential cross sections (in units of $a_0^2\,\mathrm{sr}^{-1}$) for $1s-3s$, $1s-3p$, and $1s-3d$ transitions at an incident electron energy of $k^2 = 4.0$ Ry. Integrated cross sections (in units of πa_0^2), σ_{3s}, σ_{3p}, and σ_{3d}, are also given. The numbers in brackets denote multiplicative powers of ten.

θ (deg)	$3s$	$3p$	$3d$	θ (deg)	$3s$	$3p$	$3d$
0	1.91[−1]	4.09	4.92[−1]	95	6.63[−4]	6.33[−4]	3.16[−5]
5	1.07[−1]	2.56	3.56[−1]	100	5.99[−4]	5.19[−4]	2.86[−5]
10	4.18[−2]	1.07	1.84[−1]	105	5.43[−4]	4.28[−4]	2.63[−5]
15	2.69[−2]	4.32[−1]	8.15[−2]	110	4.94[−4]	3.59[−4]	2.35[−5]
20	2.06[−2]	1.73[−1]	3.28[−2]	115	4.49[−4]	3.09[−4]	2.08[−5]
25	1.39[−2]	6.98[−2]	1.22[−2]	120	4.09[−4]	2.74[−4]	1.81[−5]
30	8.39[−3]	2.99[−2]	4.32[−3]	125	3.73[−4]	2.51[−4]	1.57[−5]
35	4.94[−3]	1.46[−2]	1.65[−3]	130	3.41[−4]	2.37[−4]	1.39[−5]
40	3.16[−3]	8.40[−3]	7.91[−4]	135	3.15[−4]	2.29[−4]	1.23[−5]
45	2.33[−3]	5.59[−3]	4.71[−4]	140	2.94[−4]	2.27[−4]	1.15[−5]
50	1.94[−3]	4.06[−3]	3.09[−4]	145	2.78[−4]	2.26[−4]	1.04[−5]
55	1.70[−3]	3.12[−3]	2.09[−4]	150	2.67[−4]	2.27[−4]	1.02[−5]
60	1.52[−3]	2.47[−3]	1.47[−4]	155	2.60[−4]	2.33[−4]	1.05[−5]
65	1.35[−3]	2.01[−3]	1.09[−4]	160	2.60[−4]	2.25[−4]	1.03[−5]
70	1.19[−3]	1.65[−3]	8.32[−5]	165	2.59[−4]	2.27[−4]	1.15[−5]
75	1.06[−3]	1.37[−3]	6.51[−5]	170	2.59[−4]	2.30[−4]	1.46[−5]
80	9.33[−4]	1.14[−3]	5.17[−5]	175	2.62[−4]	2.24[−4]	1.69[−5]
85	8.27[−4]	9.40[−4]	4.21[−5]	180	2.62[−4]	2.30[−4]	1.74[−5]
90	7.39[−4]	7.74[−4]	3.56[−5]				
σ_{3s}	1.11[−2]						
σ_{3p}	1.21[−1]						
σ_{3d}	1.91[−2]						
sum	1.51[−1]						

Table IV. As was observed previously, the angular dependence of these quantities is quite similar to that of the corresponding parameters for $2p$ excitation at the same energy. Consequently, we illustrate these results graphically only for $k^2 = 4.0$ Ry, where comparison with the measurements and calculations of Williams, Stelbovics, and Bray, [29] is possible. The agreement with experiment is reasonably good, but can be tested only at small angles. The agreement between the theoretical calculations is fairly good at all angles. Some small differences between the two sets of theoretical results presumably arise from the different sets of pseudostates employed in the expansion of the target wave function.

In addition to the measurements of Williams, Stel-

TABLE IV. Alignment parameters λ, R, and I for the $3p$ state at an incident electron energy of $k^2 = 4.0$ Ry.

θ (deg)	λ	R	I	θ (deg)	λ	R	I
0	1.000	0.000	0.000	95	0.707	0.051	0.311
5	0.710	0.318	-0.043	100	0.698	0.082	0.309
10	0.433	0.342	-0.073	105	0.699	0.114	0.299
15	0.331	0.317	-0.098	110	0.708	0.142	0.285
20	0.315	0.297	-0.132	115	0.725	0.166	0.267
25	0.353	0.280	-0.176	120	0.741	0.182	0.250
30	0.450	0.259	-0.221	125	0.758	0.192	0.234
35	0.604	0.230	-0.239	130	0.768	0.197	0.223
40	0.768	0.193	-0.209	135	0.779	0.197	0.216
45	0.893	0.151	-0.142	140	0.786	0.197	0.210
50	0.962	0.107	-0.060	145	0.796	0.191	0.206
55	0.984	0.066	0.021	150	0.810	0.184	0.199
60	0.972	0.031	0.093	155	0.834	0.176	0.186
65	0.938	0.003	0.154	160	0.872	0.152	0.172
70	0.892	-0.013	0.204	165	0.913	0.133	0.139
75	0.843	-0.018	0.244	170	0.957	0.099	0.096
80	0.797	-0.012	0.273	175	0.987	0.055	0.052
85	0.757	0.002	0.294	180	1.000	0.000	0.000
90	0.728	0.024	0.307				

TABLE V. Differential cross sections (in units of $a_0^2\,\mathrm{sr}^{-1}$) for excitation of magnetic sublevels of the $3d$ state at $k^2 = 4.0$ Ry. Integrated cross sections (in units of πa_0^2) are also given. The numbers in brackets denote multiplicative powers of ten.

θ (deg)	$3d_0$	$3d_1$	$3d_2$	θ (deg)	$3d_0$	$3d_1$	$3d_2$
0	4.92[−1]	0.00	0.00	95	9.00[−6]	5.65[−6]	5.64[−6]
5	2.13[−1]	6.64[−2]	4.98[−3]	100	8.86[−6]	5.10[−6]	4.78[−6]
10	4.89[−2]	5.44[−2]	1.31[−2]	105	9.57[−6]	4.47[−6]	3.88[−6]
15	1.24[−2]	2.44[−2]	1.01[−2]	110	1.04[−5]	3.54[−6]	3.00[−6]
20	4.15[−3]	9.16[−3]	5.18[−3]	115	1.13[−5]	2.56[−6]	2.19[−6]
25	2.01[−3]	2.98[−3]	2.12[−3]	120	1.14[−5]	1.81[−6]	1.51[−6]
30	1.26[−3]	7.80[−4]	7.54[−4]	125	1.10[−5]	1.41[−6]	9.76[−7]
35	8.38[−4]	1.55[−4]	2.52[−4]	130	1.02[−5]	1.30[−6]	5.80[−7]
40	5.36[−4]	3.93[−5]	8.79[−5]	135	9.01[−6]	1.34[−6]	3.28[−7]
45	3.22[−4]	3.93[−5]	3.54[−5]	140	8.52[−6]	1.31[−6]	1.75[−7]
50	1.79[−4]	4.71[−5]	1.75[−5]	145	7.92[−6]	1.12[−6]	1.06[−7]
55	9.48[−5]	4.63[−5]	1.08[−5]	150	8.03[−6]	1.00[−6]	7.37[−8]
60	5.10[−5]	3.96[−5]	8.51[−6]	155	8.80[−6]	7.91[−7]	7.39[−8]
65	3.16[−5]	3.03[−5]	8.11[−6]	160	9.08[−6]	5.42[−7]	5.39[−8]
70	2.36[−5]	2.15[−5]	8.32[−6]	165	1.07[−5]	3.93[−7]	1.59[−8]
75	1.92[−5]	1.45[−5]	8.40[−6]	170	1.41[−5]	2.61[−7]	2.17[−9]
80	1.55[−5]	1.01[−5]	8.01[−6]	175	1.68[−5]	6.91[−8]	1.12[−10]
85	1.23[−5]	7.61[−6]	7.32[−6]	180	1.74[−5]	0.00	0.00
90	1.01[−5]	6.27[−6]	6.50[−6]				
σ_{3d_0}	6.77[−3]						
σ_{3d_1}	4.63[−3]						
σ_{3d_2}	1.52[−3]						

bovics, and Bray [29] concerning the $3p$ state, there are earlier angular correlation measurements of Chwirot and Slevin [7]. These do not agree with the measurements of Williams, nor with either set of calculations.

Some measurements have been made of angular correlation parameters associated with the $3d$ state. Williams, Kumar, and Stelbovics [8] measured angular correlation involving sequential cascading photons to determine partial cross sections for the excitation of the $3s$ state and the magnetic substates ($m = 0, 1, 2$) of the $3d$ state integrated over angles for an incident energy of 290 eV. This energy is beyond the scope of this paper. However, we have decided to include here our results for differential cross sections for the $3d$ sublevels at $k^2 = 4.0$ Ry. These are given in Table V.

Chwirot and Slevin [7] observed that information concerning several state multipoles connected with $3d$ excitation could be obtained from measurements of L_α cascade photons emitted in coincidence with scattered electrons which had lost 12.1 eV. They determined the state multipoles s_{20}, s_{21}, and s_{22} at angles of 20° and 25° for incident energies of 54.4 and 100 eV. In a subsequent paper, Farrell *et al.* [30], the circular polarization of the L_α photon was measured. Subsequently, the derivations of formulas relating the observations to the inferred multipoles were criticized by Stelbovics, Kumar, and Williams [31]. The measurements of circular polarization were repeated with better statistics by Kumar, Stelbovics, and Williams [9] for 54.4 eV incident energy. In Fig. 22, we

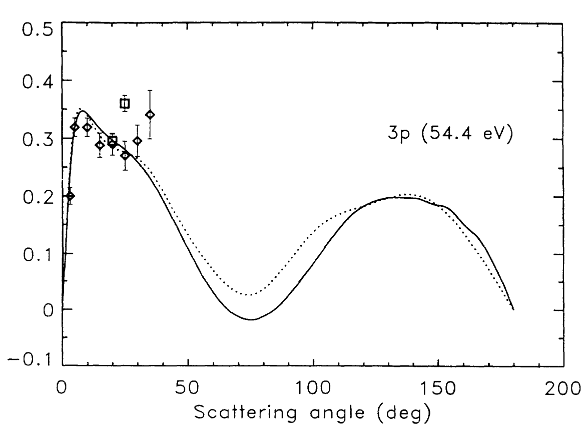

FIG. 20. Similar to Fig. 19 but for the R parameter.

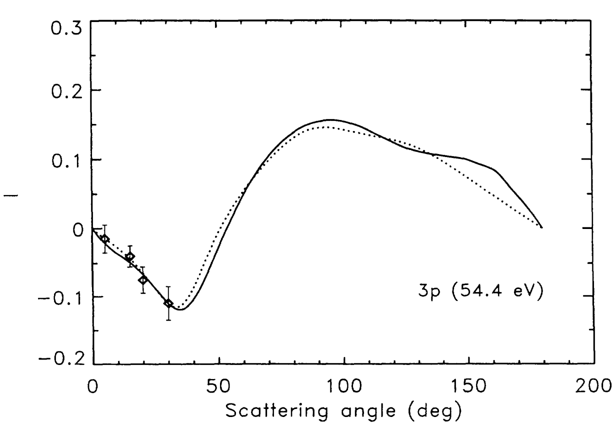

FIG. 21. Similar to Fig. 19 but for the I parameter. Ref. [7] does not contain results for this case.

TABLE VI. Calculated values for normalized state multipoles. Experimental data are from Chwirot and Slevin [7].

		Experiment		*Theory*	
E (eV)		$\theta = 20°$	$\theta = 25°$	$\theta = 20°$	$\theta = 25°$
54.4	s_{20}	-0.435	-0.072	-0.048	-0.033
	s_{21}	-0.525	-0.666	-0.330	-0.335
	s_{22}	-0.533	-0.448	-0.102	-0.044
100	s_{20}	-0.181	0.603	0.091	0.101
	s_{21}	-0.761	-0.404	-0.301	-0.317
	s_{22}	-0.715	-0.570	-0.147	-0.059

show our results for the relative Stokes parameter P_3, which we compare with those of Kumar, Stelbovics, and Williams [9].

Our results are obtained using Eqs. (16) and (17) of [9], as well as the sign convention in that paper. As in [9], we show two curves, the solid line corresponding to 500 ns time delay in the measurements, the dashed line corresponding to 45 ns. It will be seen that a small negative value is obtained for P_3 at large angles. There is a pronounced dip in the theoretical results at small angles which is not found in the experimental data. Kumar, Stelbovics, and Williams [9] compared their results with a six-state close coupling calculation which also shows a major dip at small angles, and appears to agree with our calculations.

The $3d$ state multipoles studied by Chwirot and Slevin [7] and Farrell *et al.* [30] are given by

$$\sigma s_{20} = \sqrt{\frac{8}{7}}\sigma_2 - \sqrt{\frac{2}{7}}\sigma_0 - \sqrt{\frac{2}{7}}\sigma_1, \tag{2}$$

$$\sigma s_{21} = -\sqrt{\frac{2}{7}}\mathrm{Re}\langle a_1^* a_0\rangle - \sqrt{\frac{12}{7}}\mathrm{Re}\langle a_2^* a_1\rangle, \tag{3}$$

$$\sigma s_{22} = \sqrt{\frac{8}{7}}\mathrm{Re}\langle a_2^* a_0\rangle - \sqrt{\frac{3}{7}}\sigma_1, \tag{4}$$

in which $\sigma = \sigma_0 + 2\sigma_1 + 2\sigma_2$ is the differential cross section from excitation of the $3d$ state. We tabulate our results for s_{20}, s_{21}, and s_{22} at angles of 20° and 25° for energies of 54.4 and 100 eV in Table VI. Our results disagree seriously with the measurement reported in [7].

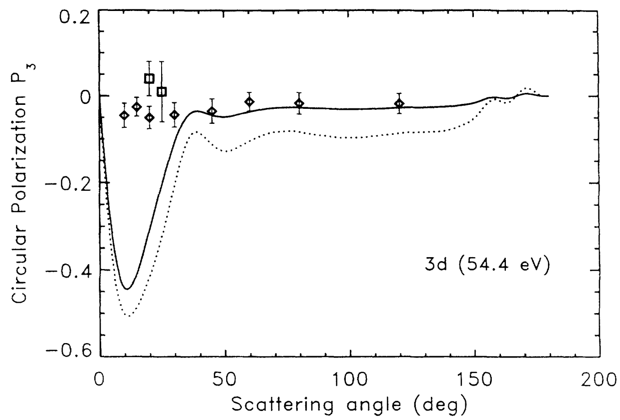

FIG. 22. Calculated Stokes parameter P_3 for L_α radiation emitted in a cascade from the $3d$ state following excitation by 54.4 eV electrons. See text for explanation of curves. Symbols: diamonds, measurements of Kumar, Stelbovics, and Williams [9]; squares, measurements of Farrell *et al.* [30].

IV. CONCLUSIONS

We have studied elastic scattering and excitation of hydrogen atoms from the ground state to the $n = 2$ and $n = 3$ states at impact energies ranging from 16 to 100 eV. In this paper, emphasis has been placed on the calculation of differential cross sections and angular correlation functions which are compared with experiment whenever possible.

We believe that the theoretical results obtained in this work are in very substantial agreement with other recent theoretical calculations which used different computational methods, all having the characteristic that contributions from continuum states of the target are included. In a sense, theoretical calculations appear to have converged for elastic scattering and $n = 2$ excitation. However, there are still some important cases of disagreement with experiment, particularly in regard to the large angle behavior of the $2p$ angular correlation functions. This is an important problem, and at this time, it seems unlikely that it will be resolved by improved theoretical calculations.

We have presented results for differential cross sections and angular correlation functions relevant to $n = 3$ excitations. Here there are far fewer opportunities for comparison with either other theory at a similar level, or with experiment. We hope that the presentation of our results will serve as a stimulus to additional experiment. This is particularly important since there are indications of potentially important disagreements between theory and experiment in regard to angular correlation functions associated with $3d$ excitation.

ACKNOWLEDGMENTS

We are indebted to Dr. Igor Bray for sending us additional numerical data concerning Refs. [5] and [29]. This research was supported in part by the National Science Foundation under Grant No. PHY 91-22117.

[1] J. Callaway and K. Unnikrishnan, Phys. Rev. A **48**, 4292 (1993).
[2] J. Callaway, K. Unnikrishnan, and D.H. Oza, Phys. Rev. A **36**, 2576 (1987).
[3] M.P. Scott, T.T. Scholz, H.R.J. Walters, and P.G. Burke, J. Phys. B **22**, 3055 (1989).
[4] I. Bray, D.A. Konovalov, and I.E. McCarthy, Phys. Rev. A **44**, 5586 (1991).
[5] I. Bray and A.T. Stelbovics, Phys. Rev. A **46**, 6995 (1992).

[6] M.P. Scott, B.R. Odgers, and P.G. Burke, J. Phys. B **26**, L827 (1993).
[7] S. Chwirot and J. Slevin, J. Phys. B **20**, 3885 (1987); *ibid.* **20**, 6139 (1987).
[8] J.F. Williams, M. Kumar, and A.T. Stelbovics, Phys. Rev. Lett. **70**, 1240 (1993).
[9] M. Kumar, A.T. Stelbovics, and J.F. Williams, J. Phys. B **26**, 2165 (1993).
[10] Y.D. Wang and J. Callaway, Z. Physik D (to be published).
[11] J. Callaway, Phys. Rev. A **32**, 775 (1985).
[12] A.E. Kingston, W.C. Fon, and P.G. Burke, J. Phys. B **9**, 605 (1976).
[13] J.F. Williams, J. Phys. B **8**, 2191 (1975).
[14] J. Callaway and J.F. Williams, Phys. Rev. A **12**, 2312 (1975).
[15] G.D. Fletcher, M.J. Alguard, T.J. Gay, V.W. Hughes, P.F. Wainwright, M.S. Lubell, and W. Raith, Phys. Rev. A **31**, 2854 (1985).
[16] D.H. Oza and J. Callaway, Phys. Rev. A **32**, 2534 (1985).
[17] J.F. Williams, J. Phys. B **9**, 1519 (1976).
[18] T.T. Scholz, H.R.J. Walters, P.G. Burke, and M.P. Scott, J. Phys. B **24**, 2097 (1991).
[19] W.C. Fon, K.M. Aggarwal, and K. Ratnavelu, J. Phys. B **25**, 2625 (1992).
[20] J. Slevin, M. Eminyan, J.M. Woolsey, G. Vassilev, H.Q. Porter, C.G. Back, and S. Watkin, Phys. Rev. A **26**, 1344 (1982).
[21] J.F. Williams, J. Phys. B **14**, 1197 (1981).
[22] J.F. Williams, Aust. J. Phys. **39**, 621 (1986).
[23] E. Weigold, L. Frost, and K.J. Nyguard, Phys. Rev. A **21**, 1950, (1980).
[24] S.T. Hood, E. Weigold, and A.J. Dixon, J. Phys. B **12**, 631 (1979).
[25] W.L. van Wyngaarden and H.R.J. Walters, J. Phys. B **19**, 929 (1986).
[26] S.N. Chormaic, S. Chwirot and J. Slevin, J. Phys. B **26**, 139 (1993).
[27] N. Andersen, J.W. Gallagher and I.V. Hertel, Phys. Rep. **165**, 1 (1988).
[28] J.F. Williams and B.A. Willis, J. Phys. B **8**, 1641 (1975).
[29] J.F. Williams, A.T. Stelbovics, and I. Bray, J. Phys. B **26**, 4599 (1993).
[30] D. Farrell, S. Chwirot, R. Srivastava, and J. Slevin, J. Phys. B **23**, 315 (1990).
[31] A.T. Stelbovics, M. Kumar, and J.F. Williams, J. Phys. B **26**, L237 (1993).
[32] See AIP document no. PAPS PLRAA-49-1854-76 for 76 pages of differential cross sections, transition amplitudes, and angular-correlation parameters. Order by PAPS number and journal reference from American Institute of Physics, Physics Auxiliary Publication Service, Carolyn Gehlbach, 500 Sunnyside Boulevard, Woodbury, New York 11797-2999. The price is $1.50 for each microfiche (98 pages) or $5.00 for photocopies of up to 30 pages, and $0.15 for each additional page over 30 pages. Airmail additional. Make checks payable to the American Institute of Physics.